Overloading of Prestressed-Concrete Spread Box-Beam Bridges

TERRY D. HAND and CELAL N. KOSTEM

ABSTRACT

An analytical scheme is developed that simulates the elastic and inelastic flexural response and the mechanism of damage initiation and propagation for prestressed-concrete spread box-beam bridges under any loading. The scheme employs the finite-element displacement method in which the nonlinear structural response is simulated by piecewise linearization of the tangent stiffness formulation. Damage initiation and propagation are simulated by dividing plate and beam elements into multiple layers, each in plane stress. The influence of box-beam torsional stiffness on the transverse flexure of the superstructure is incorporated into the model by introducing rod finite elements possessing the St. Venant torsional rigidity of the actual box section into the plane of the bridge slab. The coupled flexural and axial components of the box-beam contribution to composite bridge action are retained in twin I-beams, each corresponding to half the box beam. The model is applied to a field-tested bridge and found to yield reasonably good, slightly conservative predictions of elastic bridge deflections and girder moments. Results of postelastic simulations of several box-beam bridges are compared with those of flexurally identical or comparable I-beam bridges. Spread box-beam bridges are found to possess superstructure stiffness and strength approximately 30 percent higher than their I-beam counterparts. The lateral distribution of moment among box girders, more favorable at elastic load levels, is maintained almost proportionately well into the inelastic range, whereas progressive and unstable concentration of moment toward the loaded girder or girders is observed in comparable I-beam superstructures.

The majority of highway bridges in the United States are periodically subjected to loads far in excess of the service loads anticipated in the design process.

Investigations have been conducted over the years by various agencies to determine the overload response of bridges and to predict the deleterious effects of overloads on the various components of the superstructure. Analytical and limited experimental investigations to date have focused on the inelastic behavior of prestressed-concrete I-beam (1,2), reinforced-concrete cellular (3), and steel multigirder bridges (4). Little is known, however, about the post-linear-elastic response of prestressed-concrete spread box-beam bridges (Figure 1).

It has traditionally been assumed that these types of bridges are somehow stronger than corresponding I-beam bridges and that if the latter are

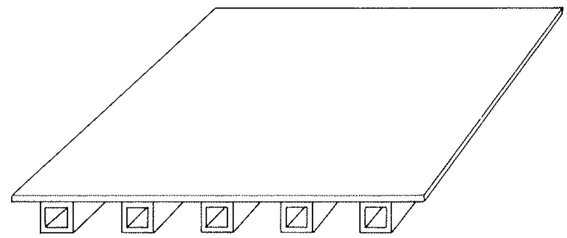

FIGURE 1 Typical prestressed-concrete spread box-beam bridge.

able to carry given loads without damage, the same should be true of similarly dimensioned box-girder bridges. This assumption has led to ambiguity among many bridge engineers as to the meaning of strength and the definition of the damage initiation mechanism for such bridges.

An analytical investigation was undertaken specifically to define the inelastic response and the mechanism of damage initiation and propagation of beam-slab prestressed-concrete spread box-beam bridges and to compare the overload characteristics of these types of bridges with those of equivalent bridges designed by using prestressed-concrete I-beams. The results clarify many questions regarding the structural response and strength differences in both the elastic and postelastic load ranges and may be used as a basis for decisions to permit overloads.

The investigation employed the finite-element displacement method. Nonlinear structural response was simulated by piecewise linearization of the tangent stiffness formulation, and damage initiation and propagation were simulated by dividing plate and beam elements into multiple layers, each in plane stress. The important influence of beam torsional stiffness on bridge behavior was incorporated into the model by introducing torsional rod elements into the plane of the slab.

DEVELOPMENT OF THE MODEL

Background

The development of a finite-element-based scheme for analysis of spread box-beam bridges proceeded from an earlier model developed principally by the second author to analyze I-beam bridges (1,2). In this model the three-dimensional elasticity problem presented by the flexure of a beam-slab superstructure was simplified and reduced to the problem of an eccentrically stiffened plate. The beam-slab bridge discretization consisted of beam and slab (plate bending and plane stress) elements. Finite-element nodes possessing in-plane (u and v) and bending (w, θ_x, and θ_y) degrees of freedom (df) are located at the middle surface of the slab (Figure 2). Coupled in-plane and bending stiffness coefficients are defined for the slab elements with respect to all 5 df, whereas major-axis bending and axial stiffness coefficients for beam elements are

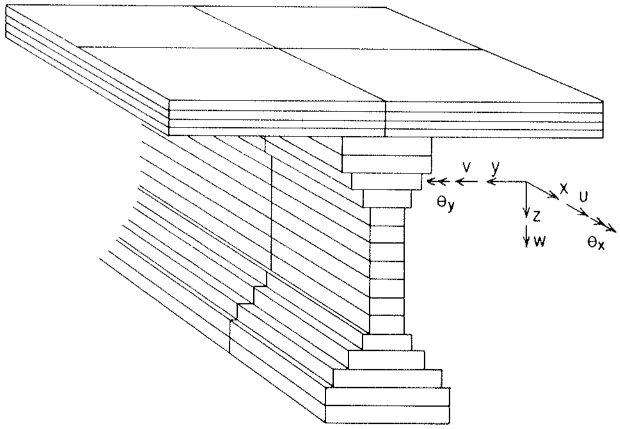

FIGURE 2 Layered beam and slab finite elements.

defined with respect only to u, w, and θ_y, thus precluding representation of weak-axis bending of the beams. Figure 2 shows the slab and beam layering scheme that allows elements to exhibit a stress variation through their depth and to experience progressive cracking, crushing, or yielding. At the same time, the layering provides the basis for redefining element stiffnesses after each load step through the appropriate summing of individual layer stiffnesses. In this scheme each layer is assumed to be in plane stress.

One of the principal shortcomings of this early model lies in its inability to incorporate the torsional stiffness of girders into the overall bending response of the superstructure. As a result, its application has been limited to bridges with beams that have negligible torsional stiffness, such as I- or T-beams. A second difficulty with the earlier model, which precluded its use in the analysis of box-beam bridges, was the question of how to treat torsional shear flows within the restricted context of the vertically layered beam stems.

Incorporation of Torsional Stiffness into the Model

Figure 3 illustrates a concept by which the torsional stiffness of box girders may be incorporated into the global stiffness of the superstructure. Notional linear finite elements, which possess the St. Venant torsional rigidity calculated for the actual box beam, are introduced longitudinally between nodes that lie over the centerline and stems of the box beams. Mathematically these elements are connected only to the θ_x df (Figure 2), which had formerly been used only in defining the transverse bending and twisting stiffnesses of the slab elements. On assembly into the global-stiffness equations, the additional stiffness provided by the torsion elements simulates the transverse stiffening effect caused by the actual beams in the real bridge. The flexural and axial stiffnesses of the box beams are retained in twin I-beams, which may continue to behave as the pure, planar beam columns of the original model.

Assumptions and Limitations

The proposed scheme for introducing the torsional stiffness of box beams into the otherwise purely flexural model necessitated several assumptions:

1. That the true torsional response of a box beam whose geometry is typical of those in the bridges under study can be reasonably approximated by St. Venant torsion alone,
2. That stresses from local transverse bending of box-beam walls in typically proportioned beams do not dominate over the primary flexural stresses and flexural and torsional shear stresses, and
3. That the usual assumptions of small deflection and small strain beam theory hold at least as well as for the original I-beam inelastic bridge model.

The first two assumptions have been validated by research by the authors and are reported elsewhere (5). The research consisted of theoretical and finite-element analyses of a box beam loaded in torsion and in combined flexure and torsion. Comparison of analytical results was made with limited benchmark data from the laboratory testing of a full-size prototype box beam (6).

The third assumption may be justified by the consideration that a bridge having torsionally stiff beams will exhibit less transverse dishing (indicative of less twisting of beams and more even distribution of moment among beams) than a bridge with flexurally equivalent but torsionally flexible beams. This implies that box beams will more closely approximate plane bending than their I-beam counterparts. Moreover, although one generally associates box sections with torsion, their vastly higher torsional strength and smaller twist angles result in lower shear strains, which when coupled with the reduced warping tendency of closed sections results in a closer adherance to the assumption of key plane sections. Last the significantly smaller deflections and curvatures exhibited by box-beam superstructures as compared with corresponding I-beam superstructures make the small deflection and small strain assumptions all the more valid.

In addition to the assumptions just stated, the bridge model, with or without the torsional elements, is limited by the inherently flexural nature of its finite-element formulation. Because transverse shear deformations and stresses are neglected, the predicted bridge response and failure mechanism

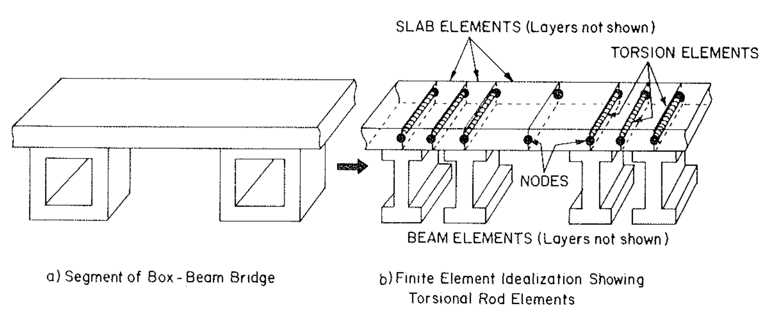

FIGURE 3 Incorporation of torsional stiffness.

is necessarily a flexural one. Thus, a bridge for which the actual overload response would lead to diagonal tension or shear cracking near the supports would be a poor candidate for analysis with this model. Because such cases are difficult to predict in advance, this model includes provisions for calculating, after each load step of the finite-element solution, the average flexural and torsional shear stress in each beam element. Torsional stresses are appropriately added or subtracted to flexural shears in each box-beam stem. Diagonal tension is then calculated, and if it approaches a preset threshold based on the rupture modulus of the concrete, the analysis is stopped. A message is printed by the computer program indicating that shear will govern the failure mechanism of the bridge, and further iterations with this model should be considered inaccurate.

VERIFICATION OF MODEL IN ELASTIC RANGE

The torsional rod element concept for simulating box-girder behavior was verified for loads in the elastic range by comparing the predicted response with corresponding measured data taken in field tests of an actual box-beam bridge (Hazleton Bridge) (7). Because measured data from the prototype were limited to midspan deflections and moment distribution coefficients derived from strain readings, an additional (elastic) finite-element model of the bridge was created to serve as a surrogate for loadings and response parameters not covered by the field tests. This second model employed a conventional finite-element package (SAP IV) and treated the bridge as a three-dimensional continuum with rectangular plate-bending elements and with membrane stiffness capability, including all parts of the slab and each wall of the girders.

Figures 4 and 5 show transverse deflection profiles at midspan as measured in the field tests versus those predicted by the SAP IV model and those predicted by the overload analysis model with special torsion elements [Bridge Overload Analysis (BOVA)]. The profiles correspond to two different transverse positions of the 333-kN (74.8-kip) test truck used in the tests (lanes 1 and 4). In each case the truck was positioned longitudinally to produce maximum bridge moment. Note that whereas the SAP IV model predicts the measured data almost exactly, the BOVA model consistently overestimates the deflection in the most heavily loaded girders.

Figures 6 and 7 show the moment distribution coefficients as derived from data taken in the field test versus values predicted by the SAP IV and BOVA

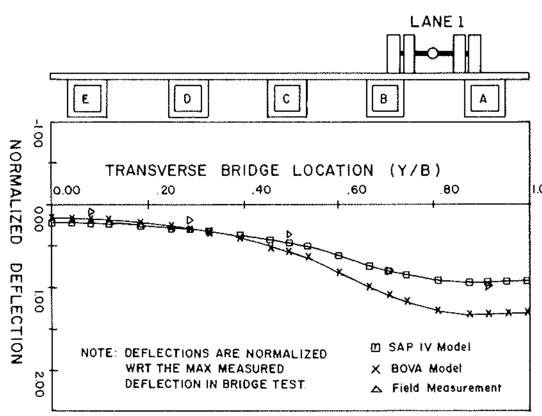

FIGURE 4 Midspan deflection profile: comparison of alternative models with test results (lane 1).

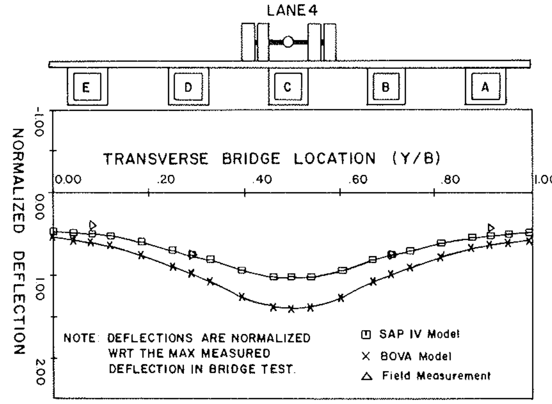

FIGURE 5 Midspan deflection profile: comparison of alternative models with test results (lane 4).

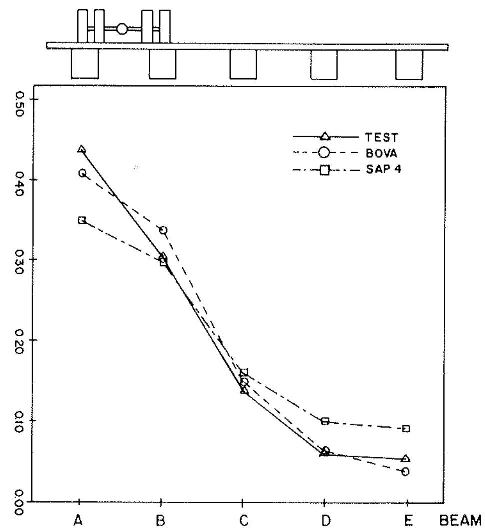

FIGURE 6 Distribution coefficients (percentage of total moment carried by beams) (lane 1).

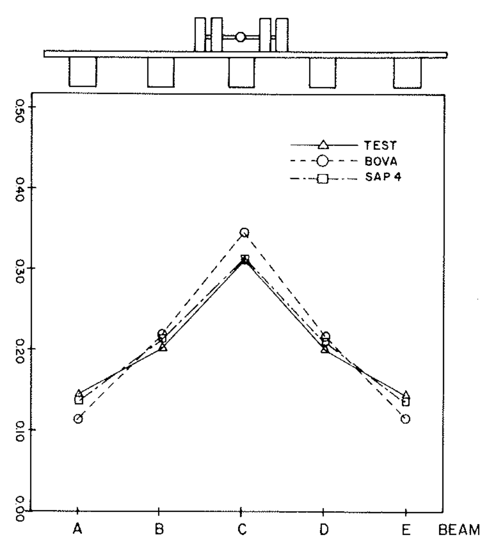

FIGURE 7 Distribution coefficients (percentage of total moment carried by beams) (lane 4).

models, respectively. These plots show good agreement generally. However, the BOVA-generated values again tend to be somewhat higher than the others, which indicates a slight overestimation of the portion of the bending moment carried by the most heavily loaded beams.

Figures 8 through 12 are longitudinal plots of

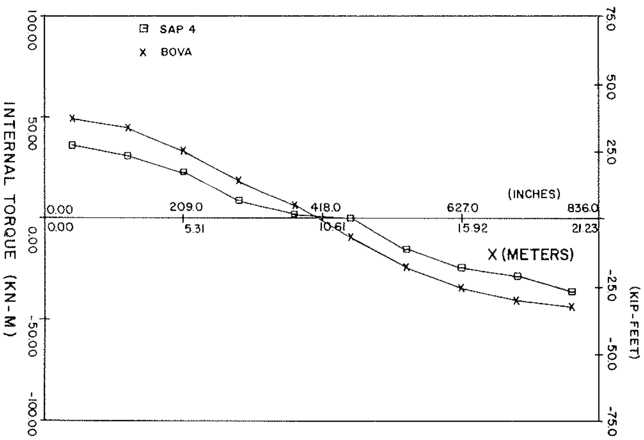

FIGURE 8 Internal torque versus longitudinal location: girder A, Hazleton Bridge (lane 2).

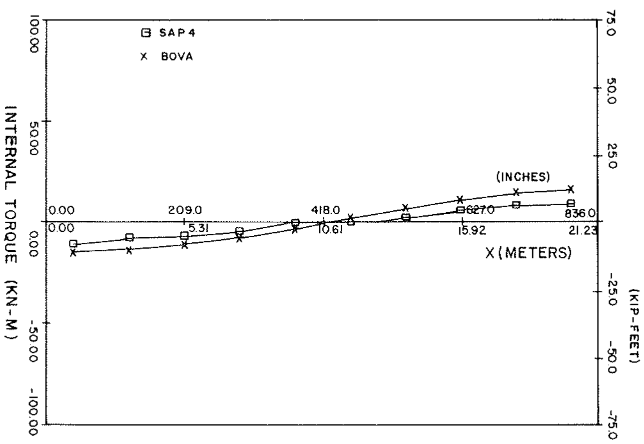

FIGURE 9 Internal torque versus longitudinal location: girder B, Hazleton Bridge (lane 2).

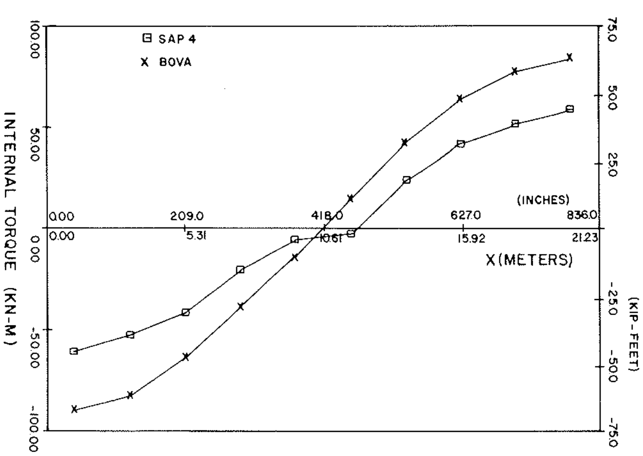

FIGURE 10 Internal torque versus longitudinal location: girder C, Hazleton Bridge (lane 2).

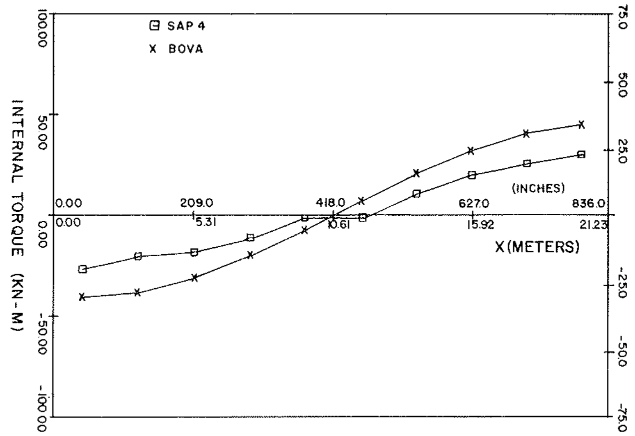

FIGURE 11 Internal torque versus longitudinal location: girder D, Hazleton Bridge (lane 2).

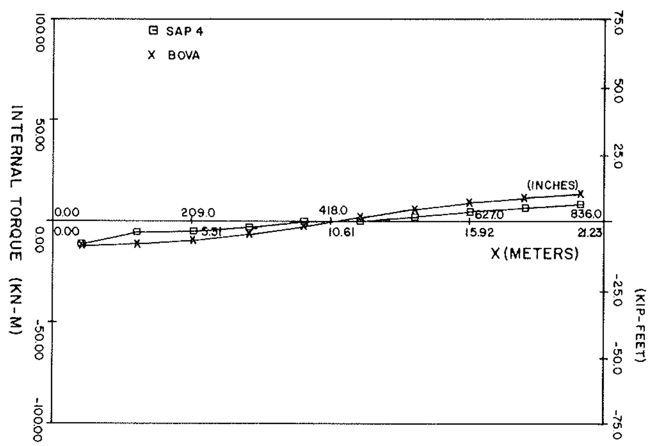

FIGURE 12 Internal torque versus longitudinal location: girder E, Hazleton Bridge (lane 2).

internal beam torque for each of beams A through E for the case of the test truck in lane 2 (straddling girder B, the second beam from the right). Note again that although the predictions of the two models show reasonable agreement on order of magnitude, the BOVA formulation again predicts larger values.

The response of the BOVA formulation for box-beam bridges (i.e., with torsion elements) is compared with that of the equivalent twin I-girder bridge (identical except without torsional elements) in Figure 13, which clearly shows the intended transverse stiffening effect contributed by the torsion elements. The loading for this plot was an AASHTO lane load in lane 2, that is, over beam B.

These results of analyses conducted at loads in the elastic range show that the response of a box-beam superstructure is quite well modeled qualitatively and reasonably well modeled quantitatively by the insertion of torsional rod elements into the layered beam-slab model as described earlier. The results suggest that in the elastic range at least, the inelastic model (BOVA) tends to overestimate somewhat the deflections, moments, and torques in the critical girder. The consistent overestimation, although problematic, is on the conservative side.

APPLICATIONS OF BOVA (BOX) IN INELASTIC RANGE

Extension of the box-beam overload model into the

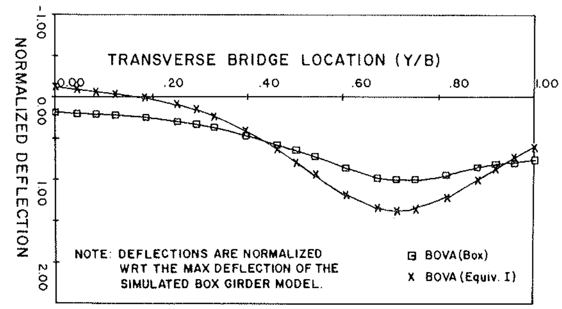

FIGURE 13 Midspan deflection profile: comparison of alternative models.

inelastic range proceeded in two stages. In the first stage the two BOVA versions of the Hazleton Bridge model (i.e., the simulated box-beam and the equivalent twin I-beam models) were each loaded to a point near the ultimate strength of the superstructure. The purpose was not only to predict the post-elastic response and failure mechanisms of the box-beam version but to investigate the differences in response between a box-beam bridge and a notional I-beam bridge identical in every detail except for the presence of the torsion elements.

The second stage involved a comparison of the responses of three distinct prestressed-concrete beam-slab bridges, each designed to Pennsylvania Department of Transportation (PennDOT) standards for the same span, width, and loading. The purpose was to evaluate the differences in behavior of actual alternative designs--bridges with eight I-beams, eight box beams, and five box beams.

Overload Analysis of Hazleton Bridge

In Figure 14 the load-deflection response of the Hazleton Bridge box-beam model is compared with that of the twin I-beam control model discussed previously. The loading consisted of monotonically in-

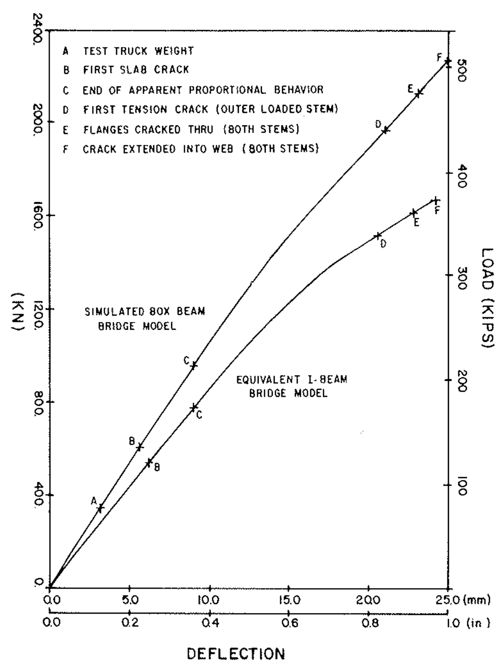

FIGURE 14 Load-deflection response of Hazleton Bridge models.

creasing patch loads corresponding to the wheel footprint of the three-axle test truck used in the field tests (7). The truck was positioned in lane 2 straddling beam B. The ordinate is the total vertical load. The abscissa is the vertical deflection at midspan on the outer stem of the loaded beam.

Critical events in the overload history of each model are annotated on the curves, and the overload simulation was stopped in each case when the predicted flexural cracks in both stems of the loaded beam extended into the bottommost web layer. In the case of the box-girder model this occurred at a load of 2,259 kN (508 kips) and a deflection of 24.2 mm (0.954 in.). At this point the curve has clearly become nonlinear but retains a large positive slope, indicating that the bridge as a whole is not yet approaching its collapse load. By comparison, the equivalent I-beam bridge revealed the same damage level at a total load of 1,077 kN (377 kips) and a deflection of 23.8 mm (0.936 in.). The slope of the curve in this case, however, has become nearly horizontal, which implies that the bridge is near its ultimate load.

Figures 15 and 16 are based on data from the same overload simulation runs but show instead the predicted midspan deflection profiles at the same total loads as those annotated on the load-deflection curves. In addition, the box-beam profile (Figure 15) has a curve for a load of 333 kN (74.8 kips), the actual test-truck weight.

Examination of the two families of curves in

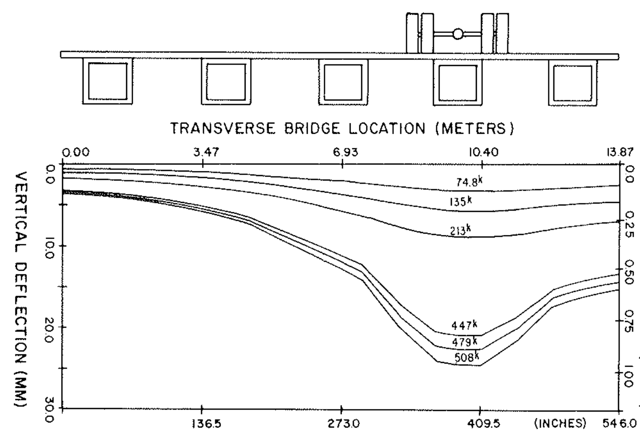

FIGURE 15 Midspan deflection profiles at various load stages: Hazleton Bridge, box-beam model.

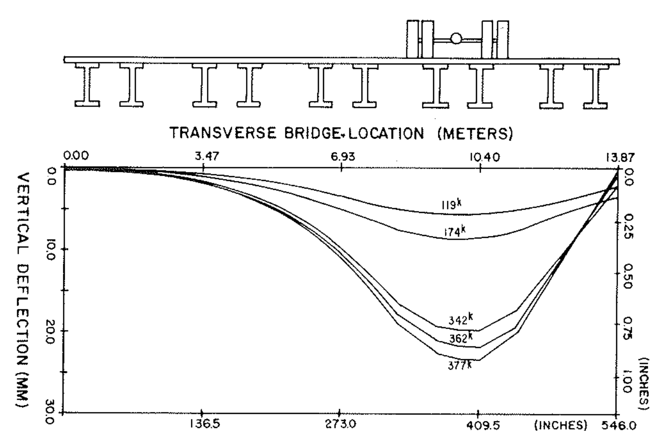

FIGURE 16 Midspan deflection profiles at various load stages: Hazleton Bridge, equivalent I-beam model.

conjunction with the load-deflection curves indicates that although critical damage occurs in both bridges at approximately the same maximum bridge deflection, the box-beam version reaches that deflection at a total load about 35 percent higher. Moreover, at this point in the equivalent I-beam bridge the loaded beam is taking on an increasing share of the total load as shown by the apparent unloading of the right-hand beam. By contrast, in the box-beam bridge the distribution of load to all beams appears to be maintained, even at high loads and severe deck and beam damage levels.

Analysis of Alternative PennDOT Bridges

The final series of analyses in the study compared the responses of three hypothetical bridges, each designed fully in accordance with PennDOT bridge standards (8) to meet the following requirements: span, 18.29 m (60 ft); total superstructure width (including curb and parapet), 14.22 m (46 ft 8 in.); and design loading, HS20 to 44, unskewed, and simply supported. From a design standpoint the bridges represent valid alternative structures with nominally equivalent capacities. These three cross sections are shown in Figure 17.

Overload simulations of the three bridges had two purposes: (a) to assess the behavior and strength differences between a typical spread box-beam bridge and an I-beam bridge having the same number of beams and beam spacing (as opposed to the equivalent I-beam version of the Hazleton Bridge, which was identical to the box-beam version except for the torsion elements but which did not represent an actual properly designed bridge) and (b) to determine differences in response between a box-beam bridge with many closely spaced small beams and one with fewer more widely spread large beams.

Figures 18, 19, and 20 show the comparative load-deflection curves and midspan deflection profiles at various load levels of the I-beam bridge and the bridge with eight box beams. The loading pattern for these analyses was a uniformly distributed lane load 3.05 m (10 ft) wide down the bridge centerline. The overload simulation was stopped at the first tension crack in the bottom flanges of the two loaded beams (both stems had to be cracked in the case of the simulated box beams).

These plots show a situation similar to the Hazleton Bridge, in which the box-beam bridge exhibits both stiffer transverse behavior and significantly greater strength. Also apparent in this comparison (not in the Hazleton Bridge) is the greater deflection capacity of the box-beam bridge at an equivalent damage level. [Actually, the box-beam bridge showed far less predicted slab damage at the 1,553-kN (349-kip) load level than the I-beam bridge showed at its 850-kN (191-kip) load level.]

The midspan deflection profiles of the bridge with eight box beams and the bridge with eight I-beams illustrate markedly different behavior at the higher postelastic load levels. In the I-beam bridge (Figure 19), what little lateral distribution of load to the exterior girders existed at the beginning appears to be degraded as (primarily) deck damage spreads. On the other hand, this lateral distribution, which is better initially in the box-beam bridge, is degraded little as deck damage propagates. Clearly the contribution of the torsional stiffness of the girders to the transverse stiffness of the superstructure maintains the transverse integrity of the system in spite of severe deck damage (Figure 20).

Figures 21 and 22 show load-deflection plots and families of midspan deflection profiles for the box-beam bridges with eight and five beams, respectively. The comparisons are not nearly so graphic or informative as the I-versus-box simulations. For these two bridge models, however, the load-deflection curves predict stiffer behavior by the five-beam bridge as opposed to greater strength and capacity for deformation in the eight-beam bridge. The loading and termination criteria were the same as those for the previous simulations. The profiles show a similar response character, particularly in regard to maintenance of lateral distribution of load.

CONCLUSIONS

In this investigation a rational analytical approach was developed for simulating the elastic and post-

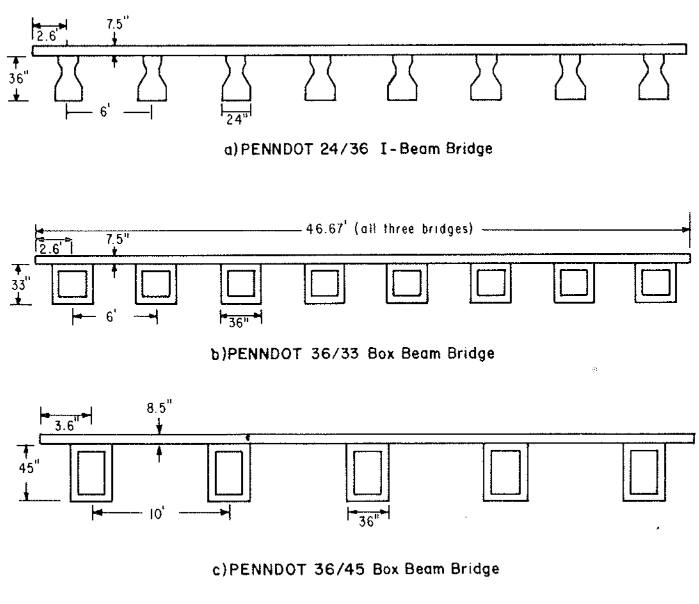

FIGURE 17 Bridge cross sections.

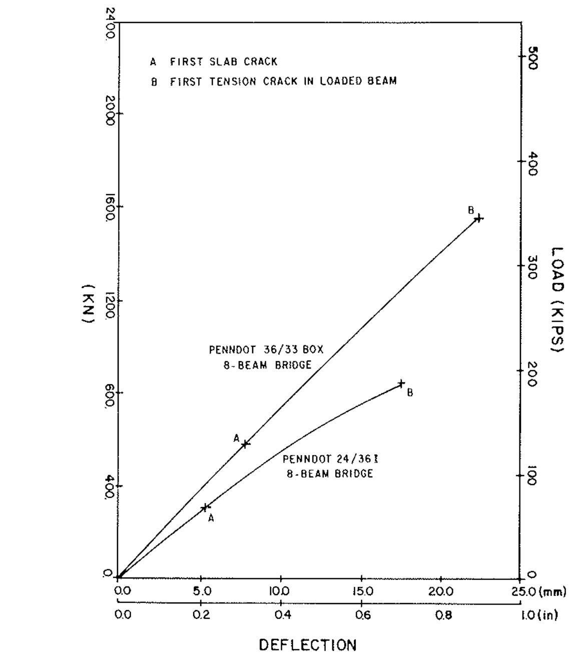

FIGURE 18 Load-deflection curves: PennDOT 36/33 box versus PennDOT 24/36 I eight-beam bridges.

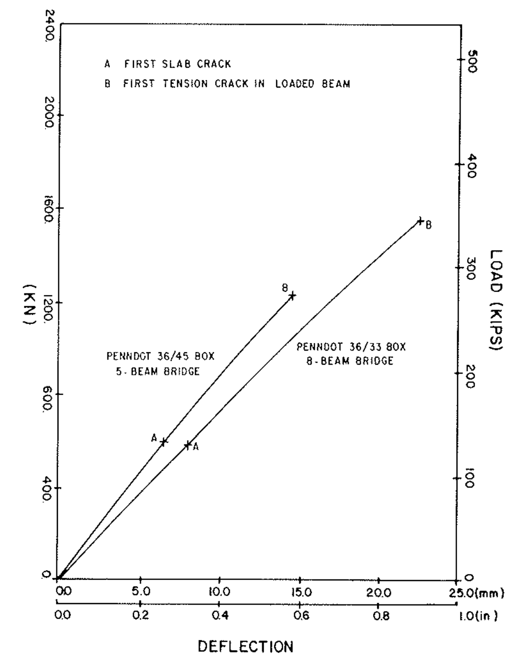

FIGURE 21 Load-deflection curves: PennDOT 36/45 five-beam versus PennDOT 36/33 eight-beam box-beam bridges.

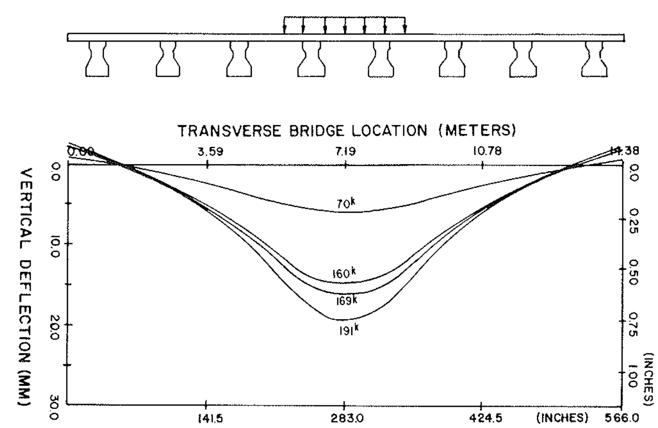

FIGURE 19 Midspan deflection profiles at various load stages: PennDOT 24/36 I-beam bridge.

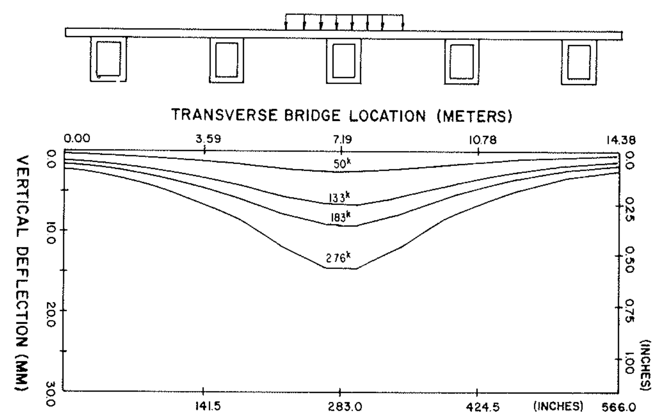

FIGURE 22 Midspan deflection profiles at various load stages: PennDOT 36/45 box-beam bridge.

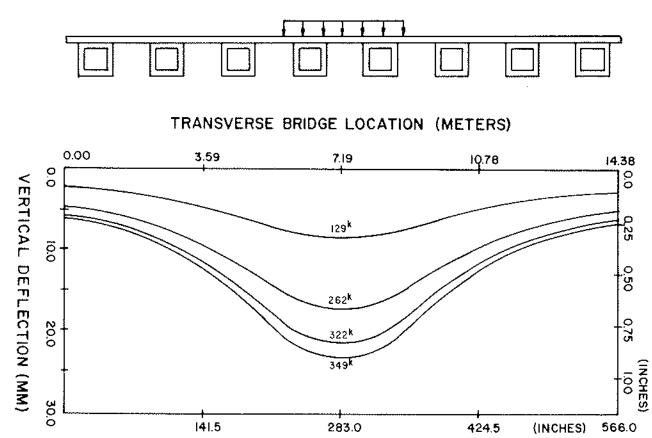

FIGURE 20 Midspan deflection profiles at various load stages: PennDOT 36/33 box-beam bridge.

elastic response of prestressed-concrete spread box-beam bridges. The scheme was shown to be a valid representation of true bridge behavior in the elastic load range, whereas its verification in the inelastic range must be deferred until prototype or scale-model bridges are tested to failure. Based on elastic studies, the model tends to err on the conservative side, suggesting that its results, extrapolated into the inelastic range, may reasonably be expected to give useful quantitative estimates of postelastic response, failure loads, and failure mechanisms.

Applications of the model to overload simulations of box-beam superstructures in comparison with equivalent or alternative I-beam superstructures suggest the following tentative conclusions:

1. Spread box-beam bridges exhibit significantly greater load-carrying capacity than their I-beam

counterparts with an identical or slightly greater major-axis moment of inertia.

2. Spread box-beam bridges exhibit higher overall flexural stiffness than comparable I-beam bridges, although the maximum bridge deflection reached at equivalent beam damage levels is about the same for the two bridge types.

3. In box-beam bridges transverse distribution of load to beams not directly loaded is higher initially and is effectively maintained through the entire load range as compared with I-beam bridges in which the initially poor transverse distribution becomes worse as total applied load is increased into the postelastic range.

REFERENCES

1. J.M. Kulicki and C.N. Kostem. The Inelastic Analysis of Prestressed and Reinforced Concrete Beams. Fritz Engineering Laboratory Report 378B.1. Lehigh University, Bethlehem, Pa., Nov. 1972.
2. W.S. Peterson and C.N. Kostem. The Inelastic Analysis of Beam-Slab Highway Bridge Superstructures. Fritz Engineering Laboratory Report 378B.5. Lehigh University, Bethlehem, Pa., March 1975.
3. J.G. Bouwkamp, A.C. Scordelis, and S.T. Wasti. Ultimate Strength of a Concrete Box Girder Bridge. Structural Division Journal of ASCE, Vol. 100, No. ST1, Jan. 1974.
4. J.C. Hall and C.N. Kostem. Inelastic Overload Analysis of Continuous Steel Multigirder Highway Bridges by the Finite Element Method. Fritz Engineering Laboratory Report 432.6. Lehigh University, Bethlehem, Pa., June 1981.
5. T.D. Hand. The Inelastic Analysis of Prestressed Concrete Spread Box Girder Highway Bridges. Ph.D dissertation. Lehigh University, Bethlehem, Pa., Sept. 1984.
6. R.M. McClure and R.M. Barnoff. Conventional and Through-Voided Box Beams Subjected to Combined Loading. In Transportation Research Record 785, TRB, National Research Council, Washington, D.C., 1980, pp. 15-21.
7. Y.L. Chen and D.A. VanHorn. Structural Behavior of a Prestressed Concrete Box-Beam Bridge--Hazleton Bridge. Fritz Engineering Laboratory Report 315A.1. Lehigh University, Bethlehem, Pa., Dec. 1970.
8. Standards for Bridge Design (Prestressed Concrete Structures). Standard BD-201. Pennsylvania Department of Transportation, Harrisburg, March 1973.

Publication of this paper sponsored by Committee on Structures Maintenance.

Overloading of Steel Multigirder Bridges

CELAL N. KOSTEM

ABSTRACT

The overloading of steel multigirder highway bridges may have deleterious effects on the structural integrity of the superstructure. The overloading of steel bridges is closely linked with the fatigue-life determination of the connection details. It is observed that the actual structural response of these bridges is different from the assumptions made in the design. Results obtained from a computer-based analytical model and simulation scheme are presented. The method provides a reliable tool to predict the linear-elastic and inelastic response of bridge superstructures up to the collapse load level. The observations from case studies have indicated that (a) interface slip between the girders and the bridge deck can be neglected for any practical overloadings, (b) high stresses due to overloading tend to be more prominent in the vicinity of the details that are prone to fatigue-crack initiation, (c) residual stresses play a nonnegligible role in the inelastic response of primary steel girders, (d) buckling is an important but not a critical phenomenon, and (e) damage initiation due to overloading can initiate in girders or in the deck, depending on the design details. It was also noted that bridges with a high degree of internal and external structural indeterminacy are less prone to damage induced by catastrophic overload.

Most highway bridges are subjected to overloading of varying degrees of severity with varying frequency. It is quite rare that all structural components of a bridge superstructure will not be subjected to stresses and deformations that will be equal to or below the values assumed by the designers. The overloading of a given bridge and its components will not necessarily occur only when a vehicle traversing the bridge is heavier than the design vehicle. Vehicles with close axle spacings, even if they are lighter than the design vehicle, can cause overloading. Thus, the issue of overloading is prevalent for all bridges. The frequency of the overloading cannot be accurately estimated unless the traffic count, including the axle spacing and weights of the axles, is monitored. Because some steel bridge components are known to be susceptible to fatigue, fatigue-crack initiation, and propagation, the overloading of steel bridges is closely related to the fatigue life of the bridges.